AN INTEGRATED PILE FOUNDATION REASSESSMENT TO SUPPORT LIFE EXTENSION AND NEW BUILD ACTIVITIES FOR A MATURE NORTH SEA OIL FIELD PROJECT

Argiolas, R.
Geotechnical Engineer, Granherne Limited, a KBR Company

Jardine, R.
Imperial College, London

Abstract
This paper considers integrated foundation reassessment and site investigation planning for a North Sea life extension and expansion project. A quantitative review of existing borehole and iterative back-analysis of recorded blow count data aided the planning of new investigations and a more reliable assessment of the new and existing platforms' foundations. The existing development comprises an FPSO and two steel jackets with skirt piles driven into predominantly very dense sands. Three of four piles driven for one jacket refused on driving and when back-analysed in conjunction with the Imperial College Pile (ICP) capacity method, the driving data indicated characteristic cone penetration test (CPT) values higher than the maxima that could be recorded with 1990s survey equipment. Subsequent investigations with higher capacity CPT cones confirmed the postulated higher q_c values and allowed pile design parameter profiles to be updated and applied, while also addressing the potential for cyclic degradation under storm loading and pile shaft capacity increase over time. The study demonstrated a good overall degree of redundancy in the jacket foundations' reserve capacities.

1. Introduction

The oil field development is located in just over 100 m water depth in the Central North Sea. The initial development, which included a Floating Production Storage and Offloading Facility (FPSO) and Wellhead Protector Platform (WPP), led to first oil in the 1990s. Further developments have taken place since first oil, including a Bridge-Linked Platform (BLP); new platform developments are now planned.

2. Borehole and platform layout

Nine boreholes, B1 to B9, were drilled between 1993 and 1996 to depths between 19.3 and 101.5 m at the locations indicated on Fig. 1, relative to the WPP and BLP jacket legs.

Eight 96" (2.438 m) Outer Diameter (OD) piles were driven in pairs (5 m apart) to 57.5 m at each leg of the WPP jacket with a Menck MHU3000 hammer. Four similar piles were driven, one at each BLP jacket leg, with an IHC S2300. The BLP piles had a target penetration of 65.3 m, but three of the four were terminated after hard driving at shallower depths of 64.8, 64.45 and 62.7 m for legs B2, B4 and D4 respectively.

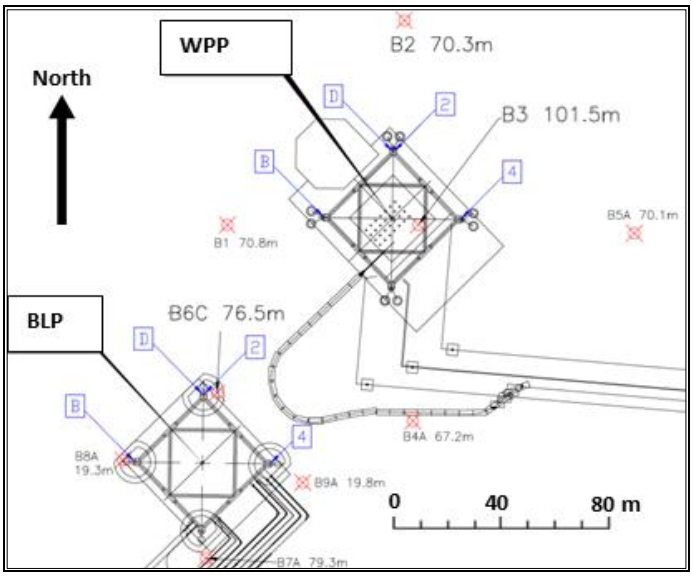

Figure 1: Platform and borehole layout

3. Geological Ground Model

The site investigations executed from 1993 to 1996 included surface/shallow-subsurface geohysics and 2D high resolution seismic geophysical surveys over the platform, subsea structure and pipeline route areas. Boreholes were advanced with downhole pushed tube sampling and in situ CPT techniques.

The ground model developed from the integrated site investigations presented in Fig. 2 comprises:

- Unit I: a thin layer of Holocene loose sand.
- Unit II: a Forth formation channel infill running southwest to northeast, comprising very soft clay, approximately 8 m thick at the platform sites, increasing to 4 m at the subsea template areas.
- Unit III, part of the Coal Pit formation, which comprises soft to very stiff sandy clay. Unit III only appears in the channel infill area.
- Units IV and V: Older Coal Pit formation sequences of Firm to Hard sandy Clay and Medium Dense to Very Dense Sand layers whose thicknesses range from 10 to 20 m and maximum depth extends to over 100 m at the platform sites.

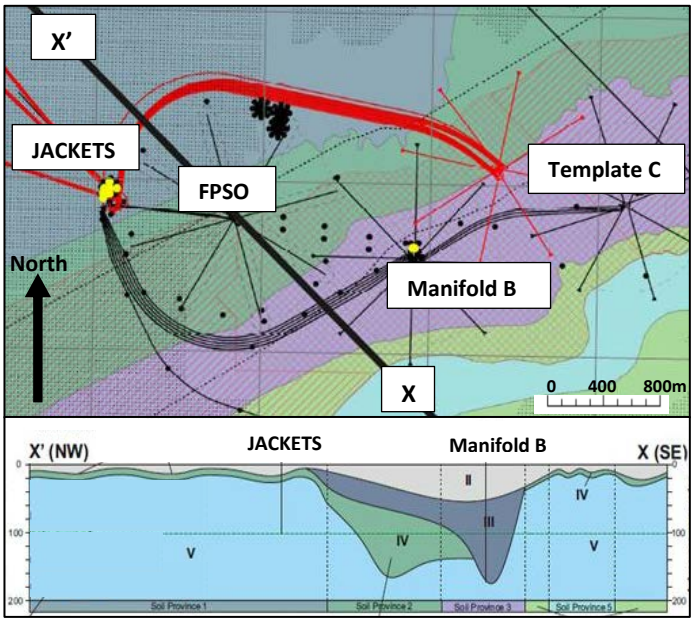

Figure 2: Ground model: map and section X'-X

4. Review of existing site investigation data

The jacket piles develop most of their axial capacity in the dense sand layers of Units IV and V. Calculations performed with CPT methods, such as the ICP (Jardine et al 2005) indicate that the axial capacities are sensitive to local variations in these Units' thicknesses, compositions and states. However, the 1993 and 1996 site investigations did not provide all the information required to undertake an ICP capacity assessment reliably. In particular:

- The CPT cones employed in the 1990s did not offer sufficient capacity to provide full q_c profiles in the densest sands (1996 q_c measurements in Fig. 6). The operators generally halted the CPT strokes when q_c exceeded 50 MPa, although some measurements were made with q_c up to 75 MPa. Measurements at other North Sea sites have shown q_c can exceed 100 MPa in very dense sands, although Jardine et al (2015) recommend treating such values cautiously.
- In the same way, the short CPT strokes that resulted from halting the CPT strokes at 'maxed-out' q_c values may have led to missing some thin sub-layers with low q_c values.
- The onshore laboratory testing involved a only limited high quality triaxial testing and no interface shear tests. Information on clay index properties and sensitivity was also sparse.

5. Back-analysis of exsiting piles' driving records

5.1 Background and back-analysis method

An iterative back-analysis was undertaken of the pile driving records to produce Soil Resistance on Driving (SRD) profiles that could be compared with ICP capacity assessments. The process started with initial 'best-estimate' local resistance estimates that were informed by judgement and lower-bound guidance charts for interface shear angles δ. Updating was then made on the basis of 1-D wave equation analyses. It is important to recognise the potential limitations of applying such tools for back-analysis, which include:

- The 1-D wave equation analysis offers only a simplified model of pile driving.
- SRD back-analysis is subject to significant uncertainty and operator dependency and cannot deliver unique inverse analyses of the soil input parameter profiles.
- The pile shaft resistances recorded during driving are likely to fall below those available in static tests. Post-installation pore pressure equalisation and other ageing processes lead to marked shaft set-up in sands and also gains in most clays.
- Pile tip driving resistances may fall far below those expected under static loading conditions.

Despite the above limitations, the back-analysis gave insights into field behaviour, particularly the BLP piles that had refused, which proved valuable in guiding new site investigations and enabling a more reliable capacity assessment. SRD was assessed using the Alm and Hamre SRD 'friction fatigue' method (1998), matching the measured blow count data with predictions from GRLWEAP, a 1-D wave equation analysis program that simulates pile response to driving. The approach considers the initial static and final residual shaft resistance values linked by a 'friction-fatigue' function, and applies soil properties which include undrained shear strength, φ' angle, CPT q_c and f_s measurements, and side and tip damping values of 0.25 and 0.50 s/m respectively. Initial 'forward predictions' were based on boreholes chosen for each pile's static capacity assessment.

Input parameters were modified interactively to improve the match between predicted and recorded blow count records.

The back-analysis results are summarised in Figs. 3 and 4 for the WPP and BLP piles respectively. The WPP traces are evidently more dispersed than the BLP equivalents. In addition, the second pile from each pair driven at the four WPP legs manifested a higher SRD than the first. This is due to the second pile penetrating into sand layers where the lateral stresses have already been raised by driving the first pile. The second pile acts, in turn, to impose additonal radial stresses on the first pile's shaft leading to a positive group action effect (in the sand layers only) as demonstrated experimentally by Chow (1997).

5.2 WPP results

The total blow counts for WPP Leg D2 were approximately half those recorded for D4 and B4, while the Leg B2 counts fell between the these limits. The backanalysed SRD profiles reflect these significant variations between piles. Considering the 57.5 m final penetration, six piles terminate in a competent, probably very dense sand, layer. Five SRDs fall in the 65-74 MN range, while one reaches an 84 MN final End of Driving (EoD) resistance.

The six WPP piles at the B2, B4 and D4 legs show broadly similar SRDs to the BLP piles driven to the same depth. However, the two Leg D2 piles show significantly lower SRDs than the other six over their full depth, with EoD values of 50 to 55 MN. Leg D2 is located between boreholes B3 and B2 of which B2 indicates a greater thickness of relatively low resistance clay. The driving records indicate that clay persisted to approximately 40 m at Leg D2, whereas the other piles encountered sand from apporximately 28m, as indicated by their closest boreholes.

The steady increases in the D2 piles' SRDs between 42-44 m and much sharper rise at 52-54 m, correlate with the presence of a dense sand layer that develops higher CPT (q_c) values. The initial forward-predicted SRD profiles generally compared well with the back-analysed profiles, except for Leg D2, as explained above. The idealised CPT profiles specified 65 MPa for q_c in the sand layers found generally between 26 m and 60 m. The pile D2 predictions were improved by abandoning the initial assumption that the spatially closest borehole, B3 should be applied to these piles, and assuming instead that the more clay-dominated second closest borehole, B2, was more applicable for the SRD and static capacity assessments.

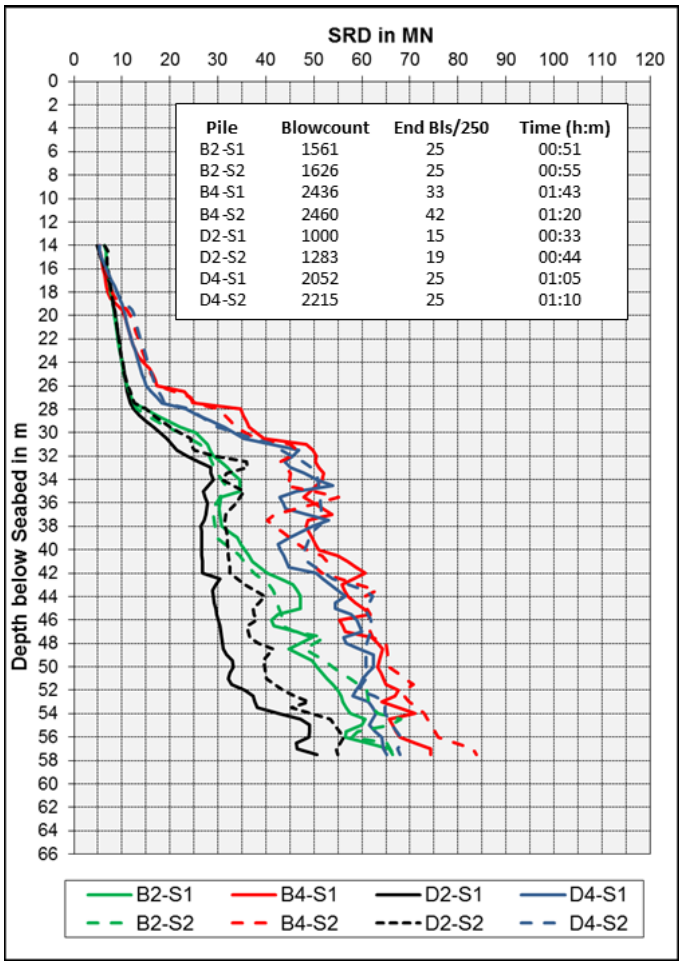

Figure 3: WPP 8-pile back-analysis results

5.3 BLP results

As shown in Fig. 4, all piles show SRD increasing with depth and rising markedly at penetrations greater than 56 m. Three of the four piles indicate EoD SRD values exceeding 100MN, close to the maximum capacity of the driving system. Only pile D2 could penetrate to its 65.3 m target depth without exceeding the blow count limit; for example Pile B4 reached a maximum of 1504 blows/250 mm over its final drive and came close to refusing at penetrations of 56.2 m and 56.45 m after electrical problems developed with the hammer that each took approximately 5.5 hours to rectify. Counts rose to 500 blows/250 mm when driving recommenced, indicating marked set-up. The back-analysed SRDs exceeded the initial estimates for the BLP piles' static capacities based on the 1990s site investigations.

The predictions and measurements could only be reconciled by assuming CPT q_c > 65 MPa over the sand sections in which the cone operators had terminated their strokes due to reaching the devices' max-out values, and so failed to achieve reliable continuous profiles. The q_c profile was adjusted upwards from 65 MPa to 80 MPa over the last 5 m of penetration within the sand layer to achieve a good blow-count match for Pile D2, which developed the

lowest final SRD at the BLP location. More radical increases in q_c were required to match the three other piles' blow counts. However, recognising the potential problems of SRD interpretation at load levels close to refusal, the latter were not adopted at the interim asessment stage.

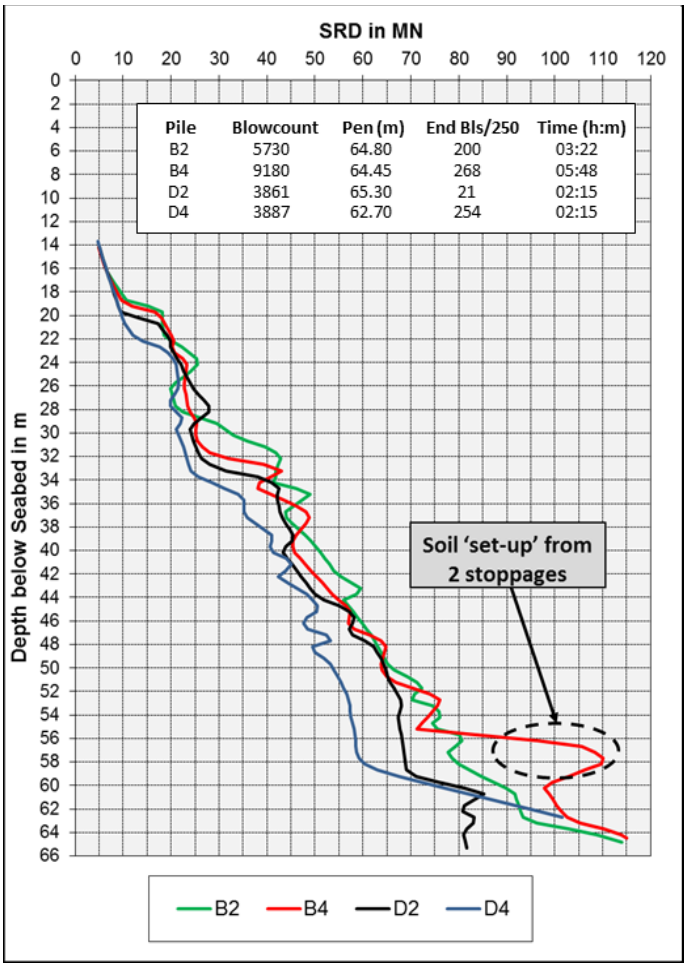

Figure 4: BLP 4-pile back-analysis results

6. Static capacity predictions

6.1 General

The original pile design undertaken in the 1990s was performed to the API main text method, which tends to underpredict axial capacity for piles with L/D<40 driven in dense to very dense sand; Jardine et al (2005). Both conditions apply at the site considered where the L/D range was 23.5-26.8 and axial capacity was dominated by very dense sands. The conservatively biased API procedures led to axial capacities of 81.5 MN and 87.0 MN for the WPP and BLP piles at their target penetrations of 57.5 m and 65.3 m respectively.

CPT-based capacity methods offer fundamental advantages in sands and have shown statistically closer predictions for pile load test databases; see Yang et al (2017). Four CPT-based methods are presented in API-RP2GEO for sands. The re-analysis adopted the ICP sand and clay methods which have been applied in multiple design and assessment studies: see Overy (2007), Aldridge et al (2010) or Merritt et al (2012).

The ICP methods rely on good quality CPT data and ring shear interface measurements of pile-surface-soil-friction angles (δ). Yield Stress Ratio (YSR) determinations are required with clays, as are reconstituted oedometer tests and/or shear strength tests to assess clay sensitivity (S_t). In the initial assessments, sand interface friction angles in sands were derived from Jardine et al (2005)'s correlations with mean particle size d_{50} values. The clay interface friction angle (δ) interpretation was based on lower bound empirical relationships between residual δ and plasticity index. Sensitivity was estimated from liquidity index, while YSR (or apparent over consolidation ratio) was estimated using SHANSEP relationships that were deemed appropriate for the clay types encountered.

Jardine et al (2015) argue that end bearing calculations should involve a consciously conservative assessement of design CPT q_c values. Noting the BLP piles' consistently hard driving to final penetration an average q_c profile was assessed for this jacket's piles over a depth range 1.5 times the pile diameter above and below the pile tip. A more cautious end bearing was adopted for WPP location due to the presence of numerous thin clay layers and the greater scatter shown by the SRD back-analysis.

Taken together, the revised shaft and base assumptions provided a conservative interim assessment of pile capacity and stiffness that allowed engineering to advance and foundation integrity to be assessed in interim re-assessments of jacket-foundation interaction. The latter adopted updated jacket in-place design loads that accounted for the higher wave loading indicated by new Metocean measurements. Meanwhile, new site investigations were planned and conducted to check the revised soil parameters, including the sand layers' q_c profiles, and so allow an updated and more secure final foundation analysis.

6.2 ICP static capacities

The unplugged ICP static capacities assessed as outlined above are presented in Tables 1 and 2, with the BLP piles showing significantly higher capacities, that reflect the cautiously raised q_c profiles and the piles' hard driving conditions.

Table 1: WPP ICP capacity predictions using SRD back-analysis results, 57.5 m penetration case

Borehole	Pile Cluster	Shaft Friction (MN)	End Bearing (MN)	ICP Comp-Capacity (MN)	ICP Tension Capacity (MN)
B1	B2	80.9	13.9	94.8	59.7
B2	D2	72.9	11.1	84.0	57.4
B3	B4, D4	80.0	13.9	93.9	60.9

Table 2: BLP ICP capacity predictions using SRD back-analysis results, final penetration cases

Borehole	Pile No. (Pen)	Shaft Friction (MN)	End Bearing (MN)	ICP Comp-Capacity (MN)	ICP Tension Capacity (MN)
B7A	B2 (64.8)	100.8	26.0	126.8	69.8
B7A	B4 (64.4)	99.0	26.0	125.0	69.5
B6C	D2 (65.3)	106.6	13.0	119.6	68.9
B7A	D4 (62.7)	98.0	26.0	124.0	69.1

6.3 SRD versus ICP capacity

The ICP 'shaft-only' capacity values are compared with those derived from the SRD back-analysis in Table 3. The last column presents the ratio of the EoD shaft SRD, as derived by back-analysis of the first pile driven for each WPP leg, to the ICP static shaft capacity.

Table 3: WPP SRD-to-static shaft capacity ratios

Piles	EoD SRD (MN)	SRD^2 - SRD^1 (MN) [A]	ICP-Comp Shaft : Base (MN)	Shaft SRD	Ratio = Shaft SRD / Shaft ICP
B2-S2 B2-S1	66.4 66.6	+0.2	80.9 : 13.9	61.8	0.76
B4-S1 B4-S2	74.4 83.8	+9.4	80.0 : 13.9	69.8	0.87
D2-S1 D2-S2	50.7 55.0	+4.3	72.9 : 11.1	47.0	0.64
D4-S1 D4-S2	65.1 68.0	+2.9	80.0 : 13.9	60.5	0.76

Note A: SRD^2-SRD^1 represents the difference in SRD between the second and first pile, driven in pairs at each jacket leg.

Following field observations by Byrne et al (2012), the shaft SRD has been computed by deducting from the total a third of the static base capacity component. The resulting ratios indicate EoD shaft SRDs that fall 13 to 36% short of the ICP estimates. However, the latter predict the static capacity available 10 days after driving. The field tests presented in Fig. 5 show that shaft capacities set-up strongly in sand and that EoD resistances can be expected to fall 10 to 40% below the medium term (nominally 10 day) ICP predictions. Table 3 lists the piles in each corner in the order in which they were installed. As noted earlier, the second pile driven in each group developed a higher SRD, with an average increment of 4.2MN (around 6%) implied in shaft resistance.

The equivalent data for the BLP piles are given in Table 4. In this case the 'EoD SRD-to-static shaft capacity ratios' are above or close to unity (100%) for three of the four piles, suggesting that their static capacity may be 20-30% higher than suggested by the 'consciously' conservative ICP calculations. This means the intial ICP static capacity has probably been underpredicted. The fourth (D2) pile's SRD was 73% of the calculated ICP static capacity, which is in line with the WPP results and Fig. 5 field load test data. This is an automatic consequence of adopting the lowest SRD pile case when re-matching the design q_c profile for the BLP static capacty estimates.

Table 4: BLP SRD-to-static shaft capacity ratios

Piles	EoD SRD (MN)	ICP-Comp Shaft : Base (MN)	Shaft SRD = SRD - ICP-Base/3	Ratio = Shaft SRD / Shaft ICP
B2	114.0	100.8 : 26.0	105.3	1.04
B4	114.9	99.0 : 26.0	106.2	1.07
D2	81.7	106.6 : 13.0	77.4	0.73
D4	101.5	98.0 : 26.0	91.5	0.95

6.4 Long term capacity

Rimoy et al (2015) discuss how the ageing trends shown in Fig. 5 continue long after full pore pressure equalization through processes that include: a) radial effective stresses increasing steadily due to creep processes relaxing circumferential arching around the shaft, b) increased shaft dilatancy developing on loading and c) physiochemical and biological activity that may impede shearing at the interface in sand and disrupt residual shear surfaces in clay.

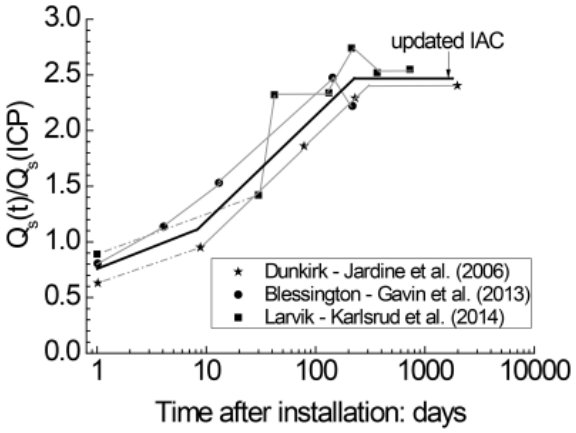

Figure 5: Field tension capacity ageing trends from ≈500mm OD steel tubular piles at sand sites, shaft capacities Qs normalized by ICP predictions. IAC is Intact Ageing Characteristic; Rimoy et al (2015).

As noted earlier, the pile driving data showed clear signs of early age set-up developing over the eleven hours of delay encountered with BLP pile B4 at around 56 m penetration. Two decades after their installation, the piles' capacities are likely to far exceed the ICP 'medium-term' values, especially within the dense sand layers. Assuming, conservatively, that little or no long-term change applies in the clay, Fig. 5 implies that for the these piles, where sands contribute up to 90% of shaft resistance, ageing in-situ may have raised shaft capacity by a factor of 2, or more. However, no gain in base resistance is expected for any of the piles.

7. New investigations and final capacity updates

New site investigations were conducted in 2014 with boreholes drilled adjacent to the existing platforms and also at the proposed new jacket location. High capacity CPT profiling was undertaken that confirmed significantly higher CPT resistances in the dense sands below BLP. As Fig. 6 indicates, q_c values in excess of 100 MPa (in red) were found in all the deep sand layers. Applying a conservatively updated q_c design line (shown in blue) led to medium term ICP capacities at least 15% greater than those listed in Tables 1 and 2.

Laboratory testign was also undertaken on soil samples, including ring shear interface tests that confirmed the original assumptions for δ in the sands and indicated higher than orginally assumed angles for the clays. However, the latter had relatively little impact on the overall axial capacities or stiffnesses.

8. Cyclic Loading

8.1 Loading response

Jardine et al (2005, 2012) emphasise the importance of considering the potentially negative effects of storm cyclic loading. The principal processes, which depend on the severity of the load cycles, include:

- Lateral pile displacements causing gapping in clays that lead to a total loss of shaft resistance over the affected shaft length.
- The soil shear straining associated with lateral cyclic deflections reducing the effective stresses and local shaft capacity;
- Axial cyclic loading subjecting the soil adjacent to the shaft to shearing that reduces the local effective stresses and so degrades local shaft capacity.

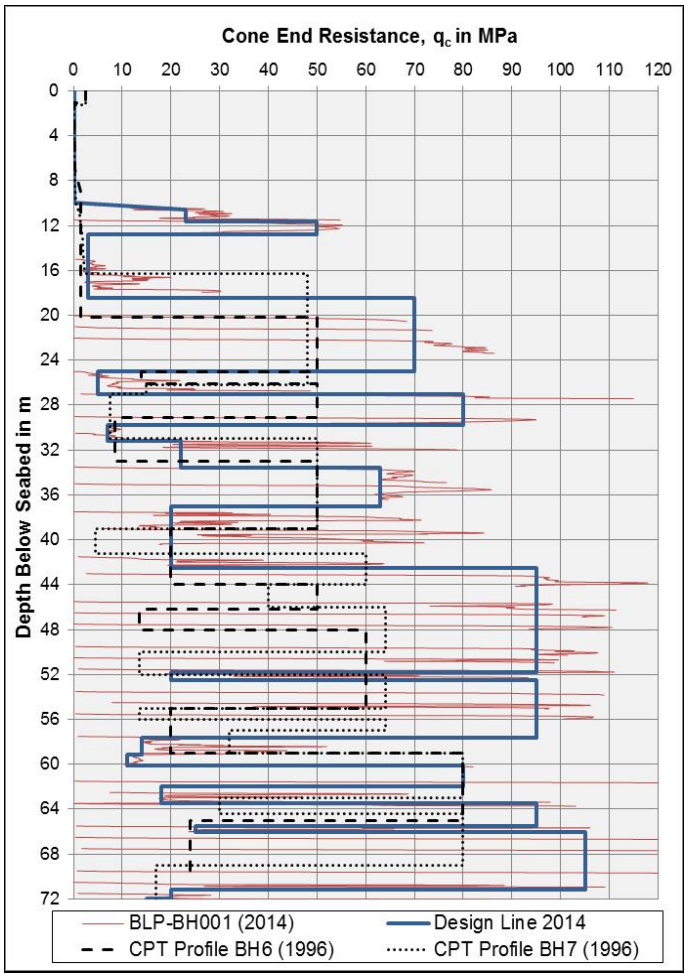

Figure 6: BLP CPT q_c versus depth from 2014 campaign, compared to the 1996 profile and interim profile based on back-analysis

8.2 Idealised Design Storm

The critical design case for this site is the 100-year storm. As recommended by Jardine et al (2012) and described by Merritt et all (2012) the loading data was treated via a rainfall procedure to sort the expected loads into 'bins' associated with fixed ranges of wave heights, as indicated in Table 5.

8.3 Lateral Cyclic Loading

Cyclic lateral loading of piles can reduce the axial and lateral stiffness of the surrounding soil over potentially significant depths below seabed. An

additional consequence can be reduced axial pile resistance within the lateral loading zone of influence.

Table 5: 100-year Idealised Design Storm

Hmax, Max. Wave Height (m)	T, Wave Period (s)	No of Cycles
20.1	11.43	1
19.5	11.25	2
18.5	10.98	4
17.5	10.62	8
16.5	10.35	15
15.5	10.17	27
14.0	10.08	131
12.0	9.99	366

The first lateral cycling issue to consider is the depth of gapping. Limited data from Clarke (1993) indicate that in tills gapping penetrates down to the depth where the maximum lateral deflection of the pile amounts to 1% of the shaft diameter (i.e. D/100). For the these piles the D/100 'gapping-limit' deflection is 24.3 mm. The expected lateral pile load-deflection response under the 100 year storm ULS event is illustrated in Fig.7 for the BLP piles. It is assumed that scour removes the Holocene sand and leaves the clay layers exposed at seabed.

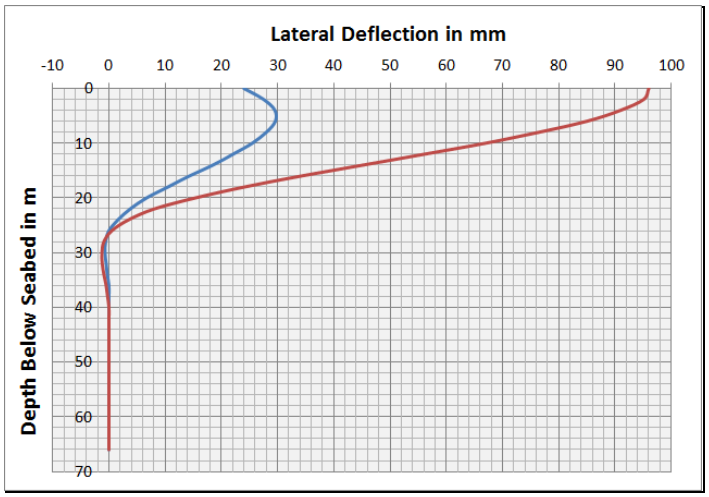

Figure 7: BLP deflections at 100-year ULS peak (red) & trough (blue) conditions; Piles D2 & B2.

The comparatively weak upper clay layers present at this site provide only slight lateral resistance and significant lateral deflections are predicted above the dense sand layers. Taking the profiles as being equally applicable to all piles at each platform, Fig.7 suggests that gapping could penetrate down to 18m below seabed. However, only the WPP D2 piles have clay strata below this 'gapping-limit' depth and gaps are unlikely to remain open in submerged sand. Assessing the depth to which cyclic damage develops below the gapping depth requires further information.

Analysis of pressuremeter unload-reload tests in glacial tills suggested a limiting deflection of D/1000, or 2.4 mm for the piles in the 'deep clay' D2 case. Fig. 7 indicates that the zero cyclic damage depth can be taken may be around 24.5 m. For simplicity, the analysis assumed a linear relationship between degradation and depth between the gapping and no-damage limits. Overall, the simplified analysis indicated that lateral cycling could be expected to reduce axial capacity over the top third of the piles' lengths. However, the loss of shaft capacity amounted to only 6 and 8% because overall capacity is dominated by the deeper sand layers.

8.4 Axial Cyclic Loading

Axial cyclic loading can degrade static shaft resistance in the absence of lateral loading. The degree of degradation depends on the severity of cyclic loading and numbers of cycles. Jardine et al (2012) summarise alternative approaches for assessing axial cyclic effects and note that interaction diagrams generated from field or model tests may be used for initial screening purposes. A chart was employed that identified global Stable, Metastable and Unstable loading limits from field tests conducted in dense North Sea sand at Dunkirk, France.

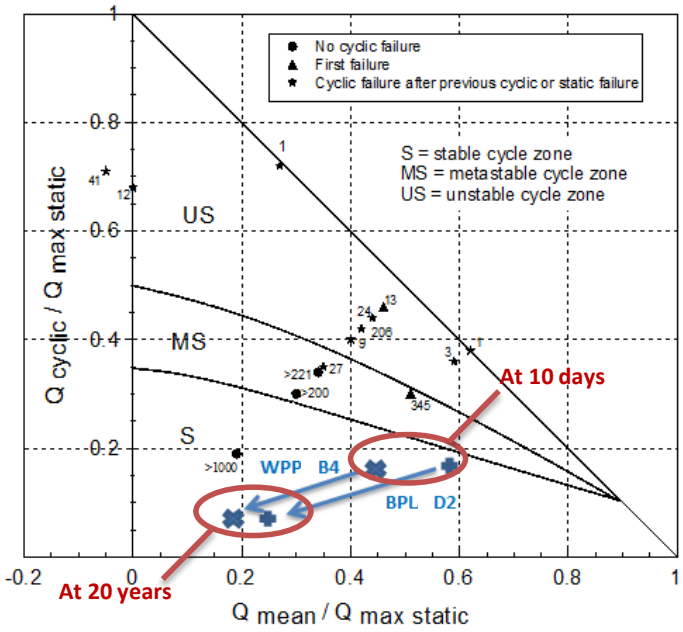

Figure 8: Limits to Stable, Metastable and Unstable regions of axial cyclic response from Dunkirk tests; Jardine et al (2012) also showing most critical BLP and WPP ULS compression-pile loading cases.

In Fig. 8, the cyclic amplitude and mean loads are normalised with respect to current shaft tension capacity, Q_t. *Stable* indicates that at >1000 cycles can be applied safely under the given normalised load combinations; capacities may even improve. *Metastable* indicates that 100s of the specified cycles

can be applied before overall shaft failure develops. *Unstable* signifies failure within 100 cycles.

Applying the 100 year storm cyclic loading data for the most critical BLP and WPP compression piles allowed the 'most severe cycle' ULS events to be plotted on Fig. 8 and related to the field test data. The ULS points plot in the *Stable* region when normalised by the medium term (nominally 10 day age) ICP capacities and move to far more stable conditions if the shaft axial capacities are assumed to grow to match the 'long term' capacity estimates. Noting that lateral cyclic effects reduce capacities by 6 to 8% and that progressive top-down failure might lead to greater degradation than was experienced by the shorter Dunkirk piles, a global 10% reduction (i.e. an additonal 2-4% axial degradation) was assumed to apply to the ICP shaft resistances to cover the combined effects of storm cyclic loading.

9. Conclusions

An integrated reassessment proved highly valuable to site investigation planning and engineering analysis for an oil field. The five main conclusions are:

1. SRD back-analyses must always be performed and interpreted cautiously. However, it proved particularly useful in identifying key aspects of field response, including the untypically low SRDs of the WPP Leg D2 piles and the effects of piling order, which may have otherwise been overlooked.
2. The SRD back-analyses for BLP justified higher interim ICP capacity estimates than the original site investigation. The 2014 site investigation subsequently confirmed the upgraded design parameters and justified more marked increases in design q_c values in the dense sand layers present.
3. The SRD backanalysis did not replace the requirement for additional site investigation, but assisted in identifying investigation requirements for both the existing and new jacket locations.
4. The potential for lateral and axial cyclic soil damage during 100 year storm loading was assessed carefully, indicating an ≈10% reduction in medium-term design shaft capacities.
5. The piles were driven up 20 years ago and are likley to have benefited from in-situ ageing processes. However, the re-analysis indicated healthy reserves of platform pile capacity under the updated Metocean regime without any need to invoke or rely on capacity growth through age.

Acknowledgments

The authors are grateful to Granherne Ltd for permission to publish this paper.

References

Aldridge, T.R., Carrington, T.M., Jardine, R.J., Little, R., Evans, T.G., Finnie, I, BP Clair Phase (2010) 'Offshore foundation design in extremely hard till', Proc 2nd Int., Symp. on Frontiers in Offshore Geotechnics, Perth, Australia.

Alm, T. and Hamre, L. (1998), 'Soil Model for Drivability Predictions' Proceedings Offshore Technology Conference (OTC) 8835.

Byrne, T., Docherty, P., Gavin, K. And Overy, R. (2012). Comparison of pile driveability methods in North Sea sand. Proc 7th Int. Conf. on Offshore Site Investigations and Geotechnics, SUT London, pp 481-488.

Chow, F.C. (1997), 'Investigations into displacement pile behaviour for offshore foundations', Ph.D, Imperial College London.

Jardine, R.J., Chow, F.C., Overy, R. and Standing, J. (2005), 'ICP design methods for driven piles in sands and clays', Thomas Telford Ltd, London.

Jardine RJ and Standing JR (2012), 'Field axial cyclic loading experiments on piles driven in sand', Soils and Foundations. 52(4): 723–737.

Jardine, R.J., Andersen, K. and Puech, A. (2012), 'Cyclic loading of offshore piles: potential effects and practical design', Keynote Paper. Proc 7th Int. Conf. on Offshore Site Investigations and Geotechnics, SUT London, pp 59-100.

Jardine, R.J., Thomsen, N.V., Mygind, M., Liingaard, M.A., C.L. Thilsted, C.L., (2015), 'Axial capacity design practice for North European wind-turbine projects', Proc 3nd Int., Symp. on Frontiers in Offshore Geotechnics, Oslo, Norway.

Merritt, A., Schroeder, F., Jardine, R., Stuyts, B., Cathie, D., Cleverly, W. (2012), 'Development of pile design methodology for an offshore wind farm in the North Sea', Proc 7th Int. Conf. on Offshore Site Investigations and Geotechnics, SUT London, pp 439-448.

Overy, R. (2007), 'The use of ICP design methods for the Foundations of Nine Platforms in the UK North Sea', Proc. 6th Int. Conf on Offshore Site Investigation & Geotechnics, SUT London, pp 359-366.

Rimoy, S.P, Silva, M. Jardine, R.J., Foray, P., Yang, Z.X., Zhu, B.T. and Tsuha, C.H.C. (2015). Field and model investigations into the influence of age on axial capacity of displacement piles in silica sands, Geotechnique, 67, 7 pp 578-589.

Yang, Z. X., Guo, W.B., Jardine, R. J. and Chow, F. C. (2017). Design method reliability assessment from an extended database of axial load tests on piles driven in sand. Canadian Geotechnical Journal. Can. Geotech. J. **54**: 59–74.